



Nuclear reaction cross sections and the optical potentials for the n - ^{12}C and N - ^{12}C scattering

In collaboration with Imane Moumene, GGI, Firenze,
now at Milano University.

Motivations to calculate reaction cross section

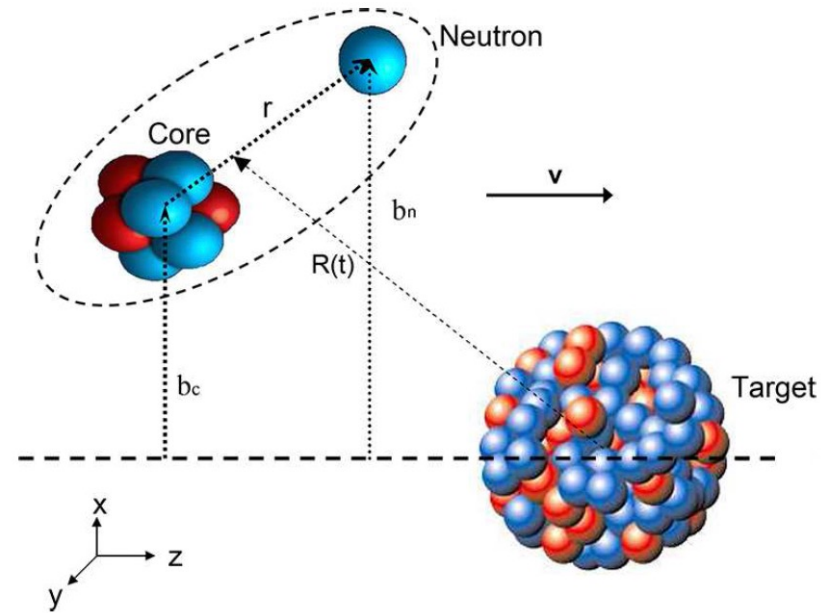
- An immediate test for the accuracy of the imaginary part of the optical potential. Plenty of data to compare to.
- Realistic nuclear reaction cross-section (σ_R) models are an essential ingredient of reliable heavy-ion transport codes. Such codes are used for risk evaluation of manned space exploration missions as well as for ion-beam therapy dose calculations and treatment planning (M. Fukuda et al.)
- From the beginning of physics with RIBs comparison of measured and calculated σ_R has been applied to deduce density distributions of exotic nuclei as well as their root mean square radii (rms). (Tanihata et al., Y. Suzuki et al....)
- Finally the core-target survival probability in knockout reactions can be fixed by reproducing σ_R .
- Predictive power of models?

Motivations to fit optical potentials

The Optical Potential (OP) is obtained from the reduction of the many body scattering problem to a one body Schrödinger equation

- A good OP can give useful information on the structure of a nucleus besides helping describing complex reactions.
- **Energy dependence of the OP**
- Phenomenological vs *microscopic* OP.
- $n+{}^9\text{Be}$
- $n+{}^{12}\text{C}$
- ${}^{12}\text{C}+{}^{12}\text{C}$ as a test
- ${}^{12}\text{C}+{}^9\text{Be}$
- ${}^{12}\text{C}$ and ${}^9\text{Be}$ are the most used targets for nuclear breakup (knockout) with RIBs

Breakup formulae



$$\sigma_{-n}^{inel} = \int d^2 \mathbf{b}_c |S_{ct}(\mathbf{b}_c)|^2 \int d^2 \mathbf{r}_\perp (1 - |S_n(\mathbf{b}_n)|^2) |\tilde{\phi}_0(\mathbf{r}_\perp)|^2$$

$$\sigma_{-n}^{el} = \int d^2 \mathbf{b}_c |S_{ct}(\mathbf{b}_c)|^2 \int d^2 \mathbf{r}_\perp |1 - S_n(\mathbf{b}_n)|^2 |\tilde{\phi}_0(\mathbf{r}_\perp)|^2.$$

See also [arXiv:2212.06056v2](https://arxiv.org/abs/2212.06056v2)

C. Hebborn, T. R. Whitehead, A. E. Lovell,³ and F. M. Nunes,

Final state interaction effects in breakup reactions of halo nuclei

A. Bonaccorso*

*Institute for Nuclear Theory, Seattle, Washington 98195-1550
and Istituto Nazionale di Fisica Nucleare, Sezione di Pisa, I-56100 Pisa, Italy[†]*

F. Carstoiu

*Institute of Atomic Physics, P.O. Box MG-6, Bucharest, Romania
(Received 1 October 1999; published 11 February 2000)*



ELSEVIER

Nuclear Physics A 706 (2002) 322–334



www.elsevier.com/locate/npe

Few-Body Syst (2016) 57:331–336
DOI 10.1007/s00601-016-1082-4



Optical potentials of halo and weakly bound nuclei

A. Bonaccorso^{a,*}, F. Carstoiu^b

A. Bonaccorso · F. Carstoiu · R. J. Charity · R. Kumar
G. Salvioni

Differences Between a Single- and a Double-Folding Nucleus-⁹Be Optical Potential

PHYSICAL REVIEW C **94**, 034604 (2016)

Imaginary part of the ⁹C - ⁹Be single-folded optical potential

A. Bonaccorso,^{1,*} F. Carstoiu,² and R. J. Charity³

Reaction cross sections at intermediate energies and Fermi-motion effect

M. Takechi,^{1,*} M. Fukuda,¹ M. Mihara,¹ K. Tanaka,² T. Chinda,¹ T. Matsumasa,¹ M. Nishimoto,¹ R. Matsumiya,¹
 Y. Nakashima,¹ H. Matsubara,¹ K. Matsuta,¹ T. Minamisono,³ T. Ohtsubo,⁴ T. Izumikawa,⁵ S. Momota,⁶ T. Suzuki,⁷
 T. Yamaguchi,⁷ R. Koyama,⁴ W. Shinozaki,⁴ M. Takahashi,⁴ A. Takizawa,⁴ T. Matsuyama,⁴ S. Nakajima,⁷ K. Kobayashi,⁷
 M. Hosoi,⁷ T. Suda,² M. Sasaki,⁸ S. Sato,⁹ M. Kanazawa,⁹ and A. Kitagawa⁹

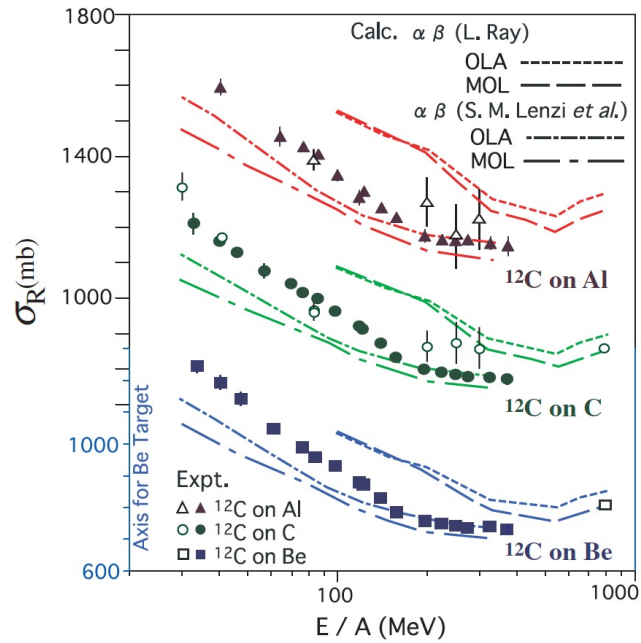


FIG. 1. (Color online) The σ_R data for ^{12}C as a function of beam energy. The closed symbols denote the present data and open symbols denote data from Refs. [8,25–27]. The OLA and MOL calculations were performed using the NN parameters from Ref. [22] (short and long dashed curves) and Ref. [23] (short and long dash-dotted curves).

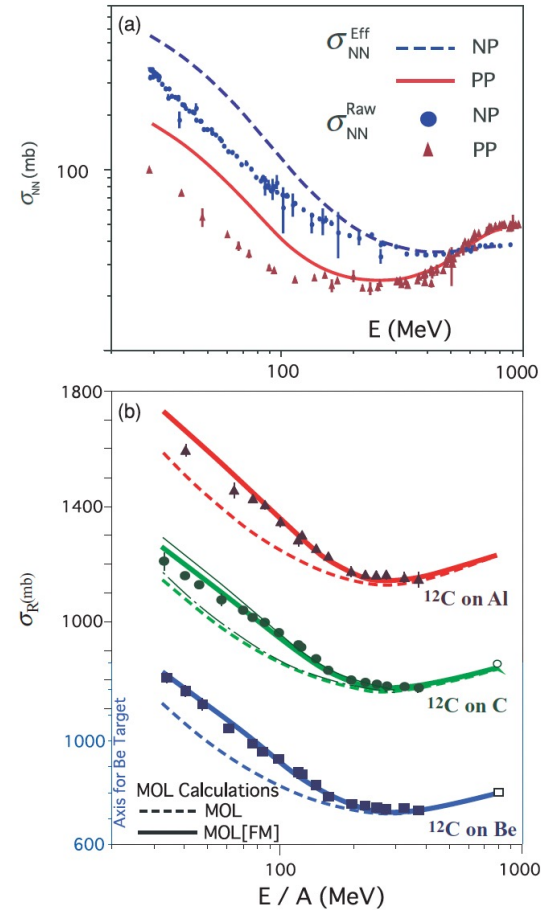


FIG. 2. (Color online) (a) Modified σ_{NN} as effective NN cross section (σ_{NN}^{eff}), which is compared with the raw σ_{NN} . (b) MOL calculations with $\beta(E)$ from Eq. (4) (dashed curve) and MOL[FM] calculations (solid curve) are compared with experimental data. We also show the MOL and MOL[FM] calculations using a Gaussian-type density for the C target (thin solid and dot-dashed curves).

N+N The Glauber reaction cross section is given by

$$\sigma_R = 2\pi \int_0^\infty b db (1 - |S_{NN}(\mathbf{b})|^2), \quad (1)$$

where

$$|S_{NN}(\mathbf{b})|^2 = e^{2\chi_I(b)} \quad (2)$$

is the probability that the nucleus-nucleus (NN) scattering is elastic for a given impact parameter \mathbf{b} .

The imaginary part of the eikonal phase shift is given by

$$\begin{aligned} \chi_I(\mathbf{b}) &= \frac{1}{\hbar v} \int dz W^{NN}(\mathbf{b}, z) \\ &= \frac{1}{\hbar v} \int dz \int d\mathbf{r}_1 W^{nN}(\mathbf{r}_1 - \mathbf{r}) \rho(\mathbf{r}_1), \end{aligned} \quad (3)$$

where W^{NN} is negative defined as

$$\mathbf{S.F.} \quad W^{NN}(\mathbf{r}) = \int d\mathbf{b}_1 W^{nN}(\mathbf{b}_1 - \mathbf{b}, z) \int dz_1 \rho(\mathbf{b}_1, z_1). \quad (4)$$

$$\mathbf{D.F.} \quad W^{NN}(\mathbf{r}) = -\frac{1}{2} \hbar v \sigma_{nn} \int d\mathbf{b}_1 \rho_p(\mathbf{b}_1 - \mathbf{b}, z) \int dz_1 \rho_t(\mathbf{b}_1, z_1). \quad (5)$$

Also

$$\mathbf{s.f.} \quad W^{nN}(\mathbf{r}) = -\frac{1}{2} \hbar v \sigma_{nn} \rho_t(\mathbf{r}) \quad (6)$$

$$\mathbf{D.F.} \quad \chi_I(\mathbf{b}) = -\frac{1}{2} \sigma_{nn} \int d\mathbf{b}_1 \int dz \rho_p(\mathbf{b}_1 - \mathbf{b}, z) \int dz_1 \rho_t(\mathbf{b}_1, z_1).$$

The double folding (5) for W^{NN} is conceptually **wrong** because the interaction acts only to first order, infact it was originally introduced for the REAL part. Eq.(4) with a phenomenological W^{nN} is in principle more accurate.

PHYSICAL REVIEW C, VOLUME 62, 034608

Scatterings of complex nuclei in the Glauber model

B. Abu-Ibrahim* and Y. Suzuki

$$\mathbf{MOL} \quad e^{i\tilde{\chi}_{OLA}(b)} = \exp\left(-\int d\mathbf{r} \rho_P(\mathbf{r}) \Gamma_{NT}(\boldsymbol{\xi} + \mathbf{b})\right),$$

$$\Gamma_{NT}(\mathbf{b}) = \sum_{k=1}^K \frac{1 - i\alpha_k}{4\pi\beta_k} \sigma_k \exp\left(-\frac{b^2}{2\beta_k}\right),$$

Phenomenological potentials

3

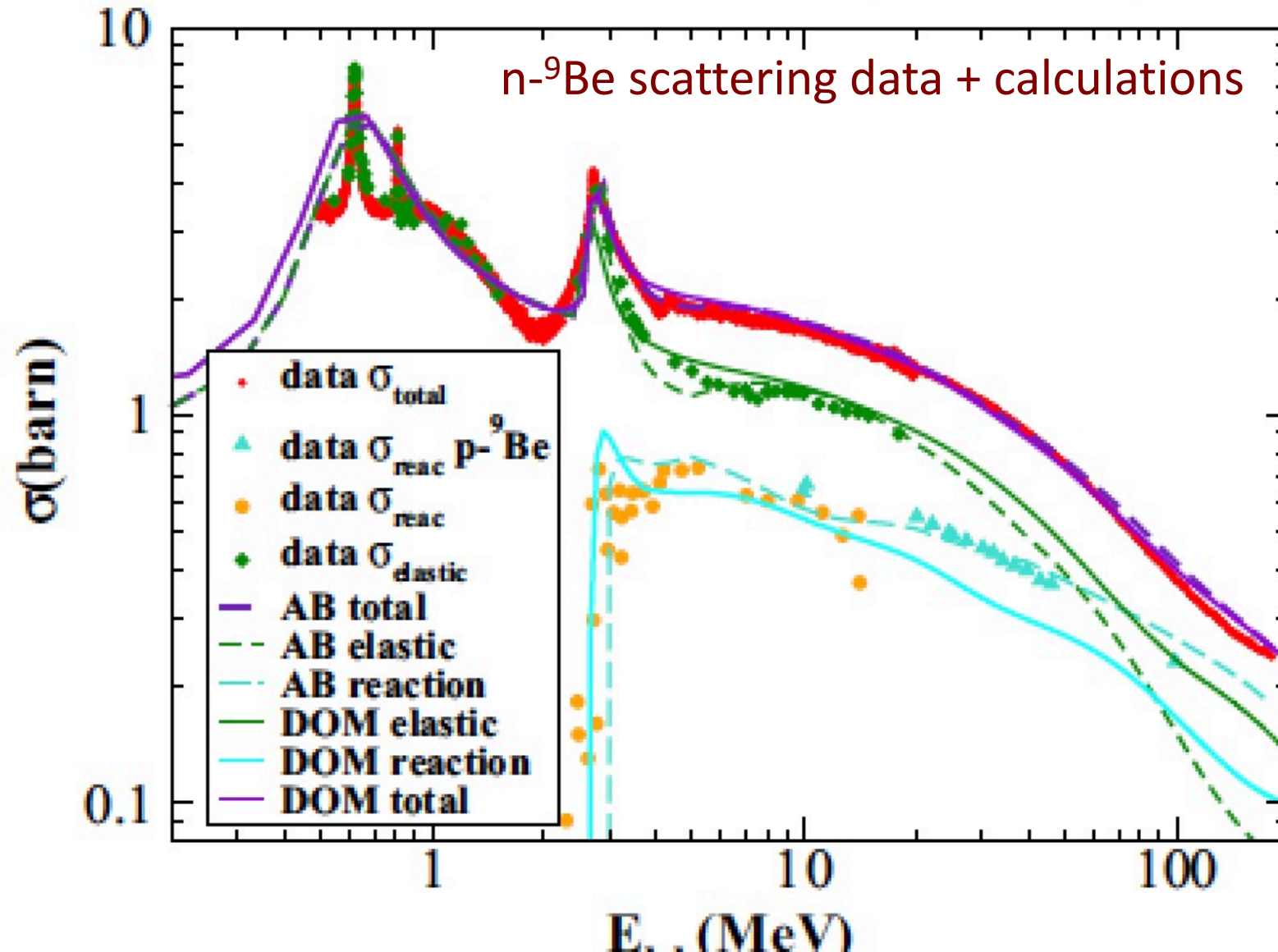
| E_{lab} (MeV) | V^R (MeV) | r_0^R (fm) | a^R (fm) | W^{sur} (MeV) | W^{vol} (MeV) |
|-----------------------------|-------------------------|------------------------------|-----------------------|-------------------------------|------------------------------|
| $20 \leq E_{lab} < 40$ | $31.304 - 0.145E_{lab}$ | $1.647 - 0.005(E_{lab} - 5)$ | $0.3 - 0.0001E_{lab}$ | $1.65 + 0.365E_{lab}$ | $5.6 - 0.005(E_{lab} - 20)$ |
| $40 \leq E_{lab} < 111$ | " | " | " | $16.25 - 0.05(E_{lab} - 40)$ | $5.5 - 0.01(E_{lab} - 40)$ |
| $111 \leq E_{lab} < 160$ | " | " | 0.288 | 12.7 | 4.8 |
| $160 \leq E_{lab} < 200$ | " | " | " | $12.7 - 0.025(E_{lab} - 160)$ | $4.8 - 0.025(E_{lab} - 160)$ |
| $200 \leq E_{lab} < 215$ | " | " | " | $11.7 + 0.02(E_{lab} - 200)$ | $3.8 + 0.02(E_{lab} - 200)$ |
| $215 \leq E_{lab} \leq 500$ | 0 | " | " | " | " |

TABLE I: Energy-dependent optical-model parameters for the (AB) potential for n+⁹Be. $r_0^I=1.3$ fm, $a^I=0.3$ fm at all energies.

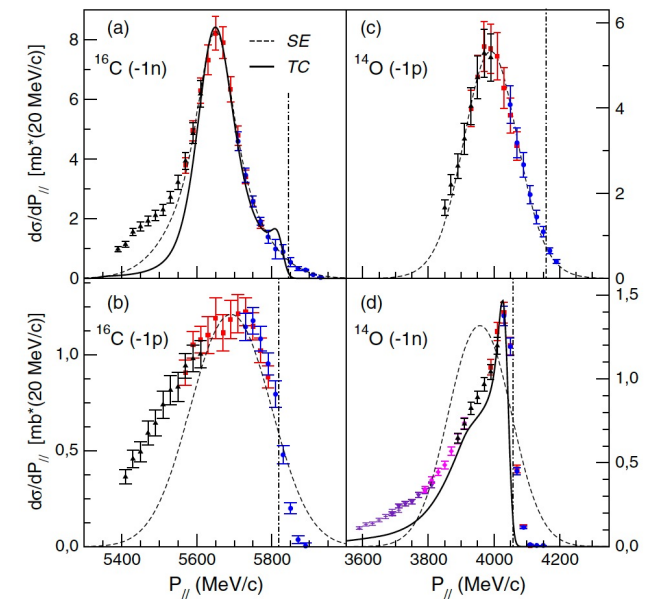
| E_{lab} (MeV) | V^R (MeV) | r_0^R (fm) | a^R (fm) | W^{sur} (MeV) | W^{vol} (MeV) |
|-----------------------------|-------------------------|------------------------------|---------------|-------------------------------|------------------------------|
| $160 \leq E_{lab} < 200$ | $31.304 - 0.145E_{lab}$ | $1.647 - 0.005(E_{lab} - 5)$ | 0.288 | $12.7 - 0.025(E_{lab} - 160)$ | $4.8 - 0.025(E_{lab} - 160)$ |
| $200 \leq E_{lab} < 215$ | " | " | " | 11.7 | 3.8 |
| $215 \leq E_{lab} < 220$ | 0 | " | " | " | " |
| $220 \leq E_{lab} \leq 500$ | " | 0.1 | " | $11.7 + 0.02(E_{lab} - 220)$ | $3.8 + 0.02(E_{lab} - 220)$ |

TABLE II: Energy-dependent optical-model parameters of the potential n-¹²C for $E_{lab} \geq 160$ MeV. At lower energies, the parametrization is the same as for ⁹Be on Table I.

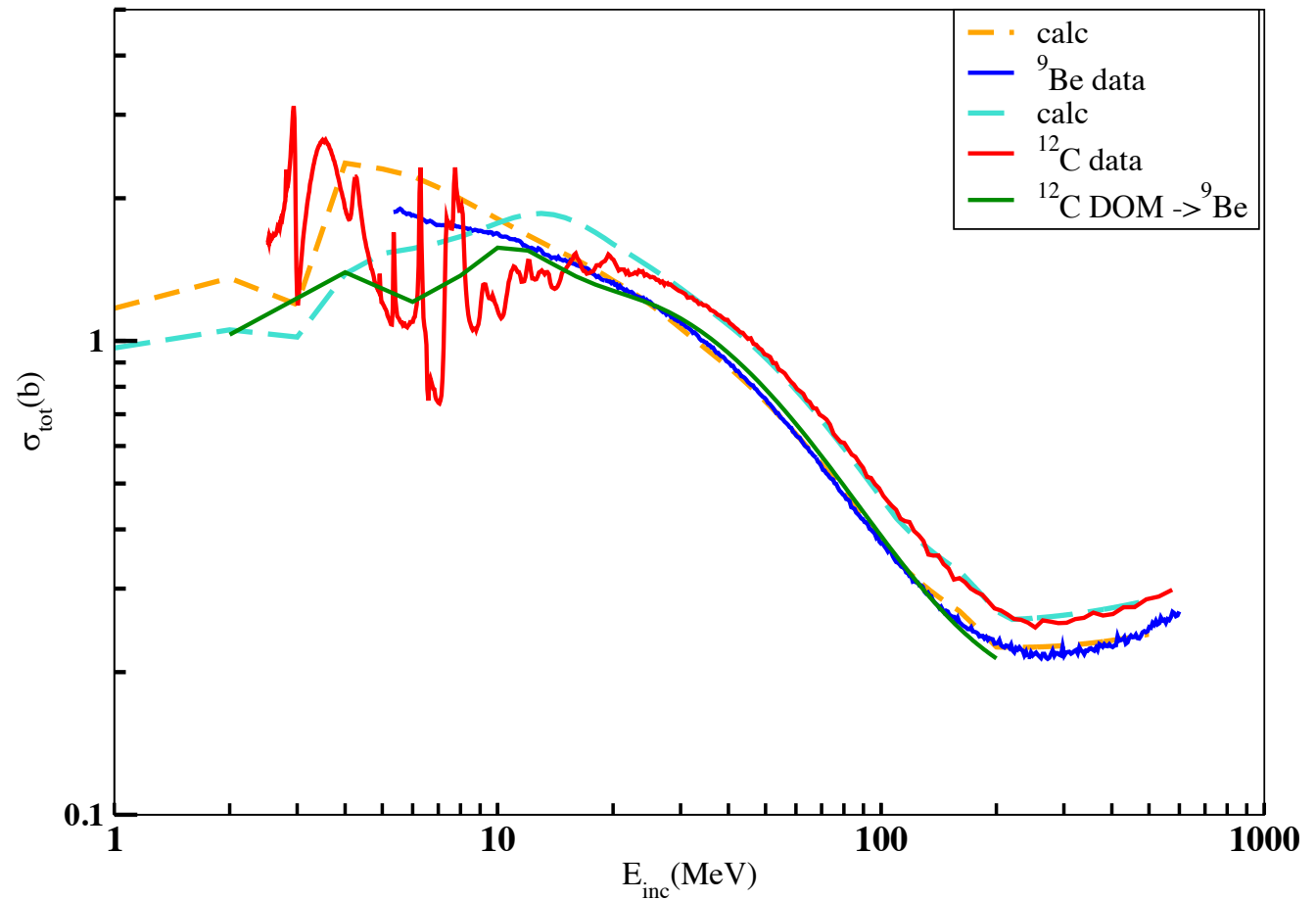
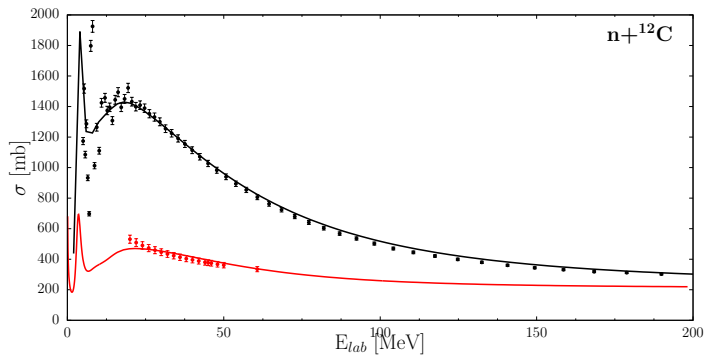
Resonances described by $\delta V(r) = 16\alpha \frac{e^{2(r-R^R)/a^R}}{(1 + e^{(r-R^R)/a^R})^4}$ consistent with dispersive contribution



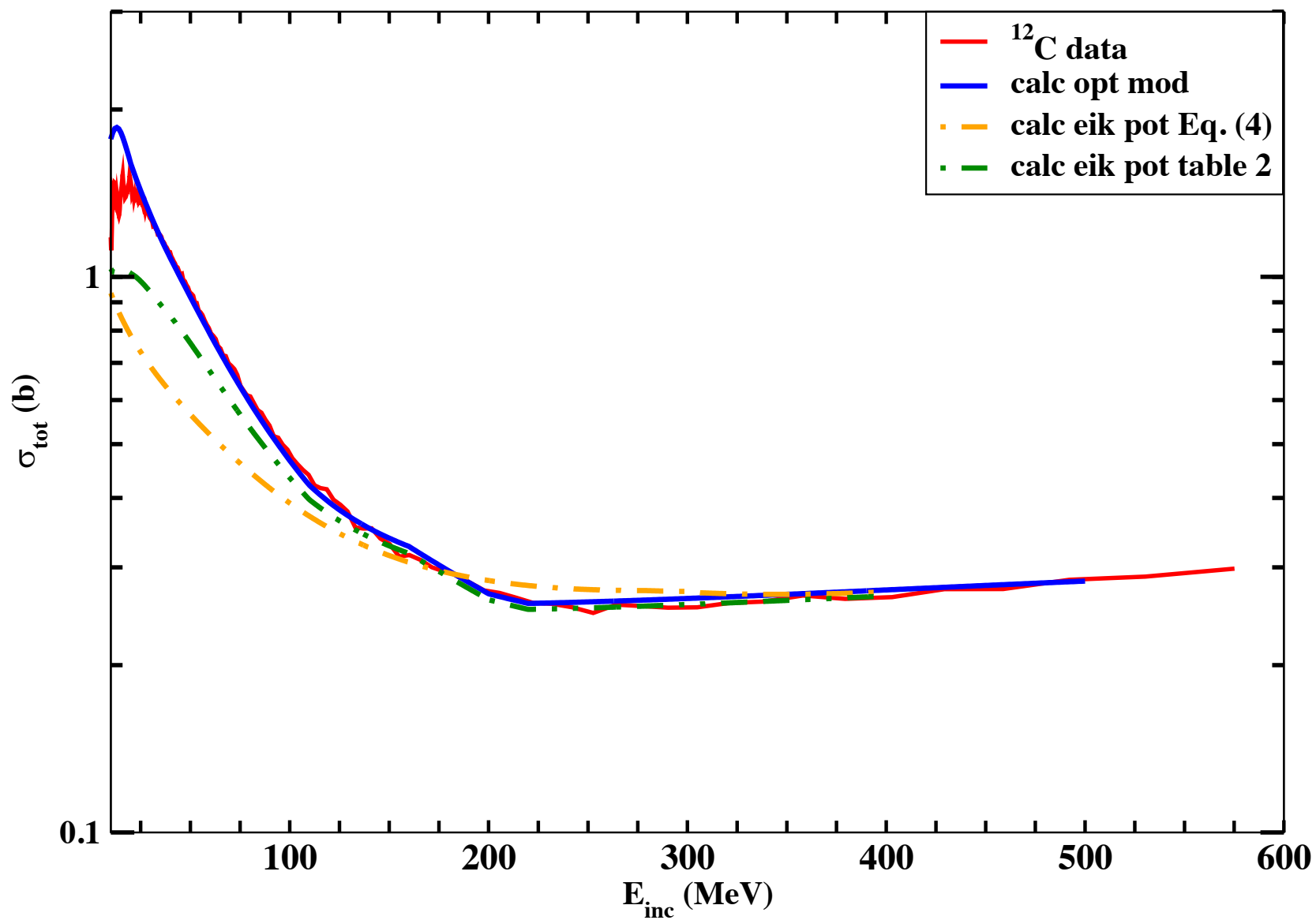
F.Flavigny et al., PRL 108, 252501 (2012)



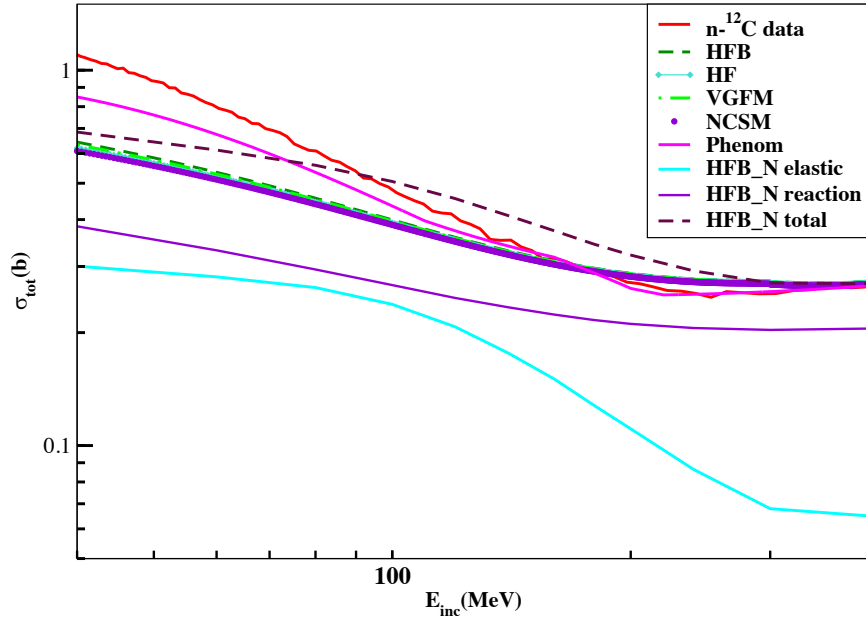
Total experimental and calculated cross sections. Lower blue symbols for ${}^9\text{Be}$, upper red symbols for ${}^{12}\text{C}$. The optical model calculations are given by the orange and cyan dashed lines, respectively. The solid green line is a calculation made with a DOM potential obtained for ${}^{12}\text{C}$ and applied to ${}^9\text{Be}$. DOM calculations (LHS) courtesy of Mack Atkinson (LLNL)



^{12}C



$n+^{12}\text{C}$, $^{12}\text{C}+^{12}\text{C}$
dominance of surface absorption



σ_{nn} can be fixed but what about α_{nn} ? HFB_N with energy dependent α_{nn} . Others with energy **independent** α_{nn}

In medium effects?

Microscopic calculation of in-medium proton-proton cross sections

G. Q. Li and R. Machleidt

Phys. Rev. C 49, 566

MOL: B. Abu-Ibrahim and Y. Suzuki, Phys. Rev. C 62, 034608 (2000).

VGFM(Wiringa) **NV2+3-IIb***

<https://www.phy.anl.gov/theory/research/density/>

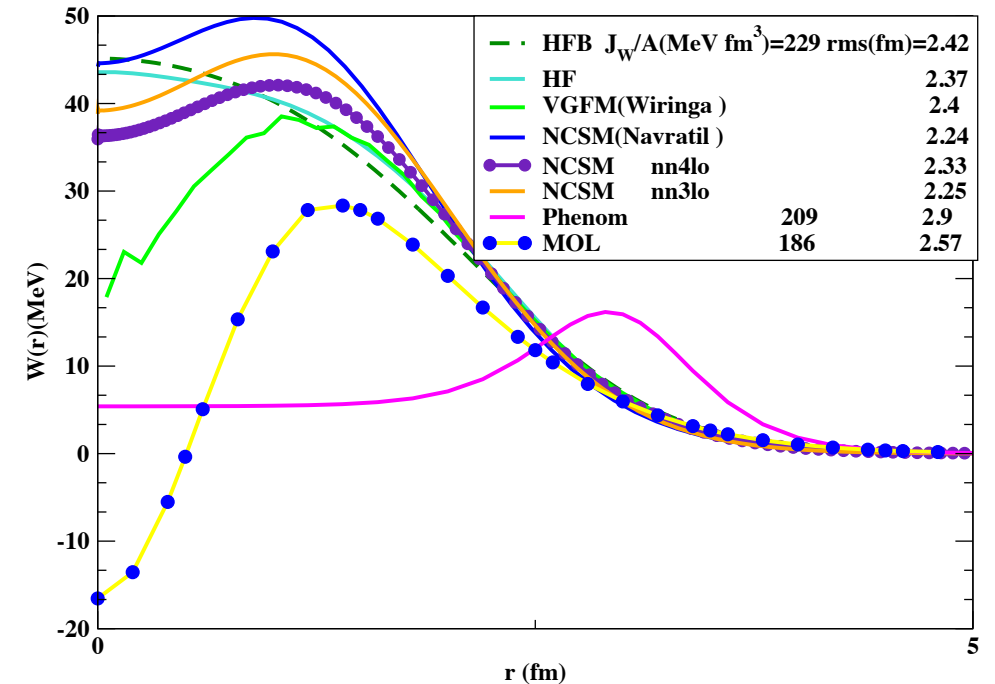
Light-Nuclei Spectra from Chiral Dynamics

M. Piarulli et al., Phys. Rev. Lett. 120, 052503

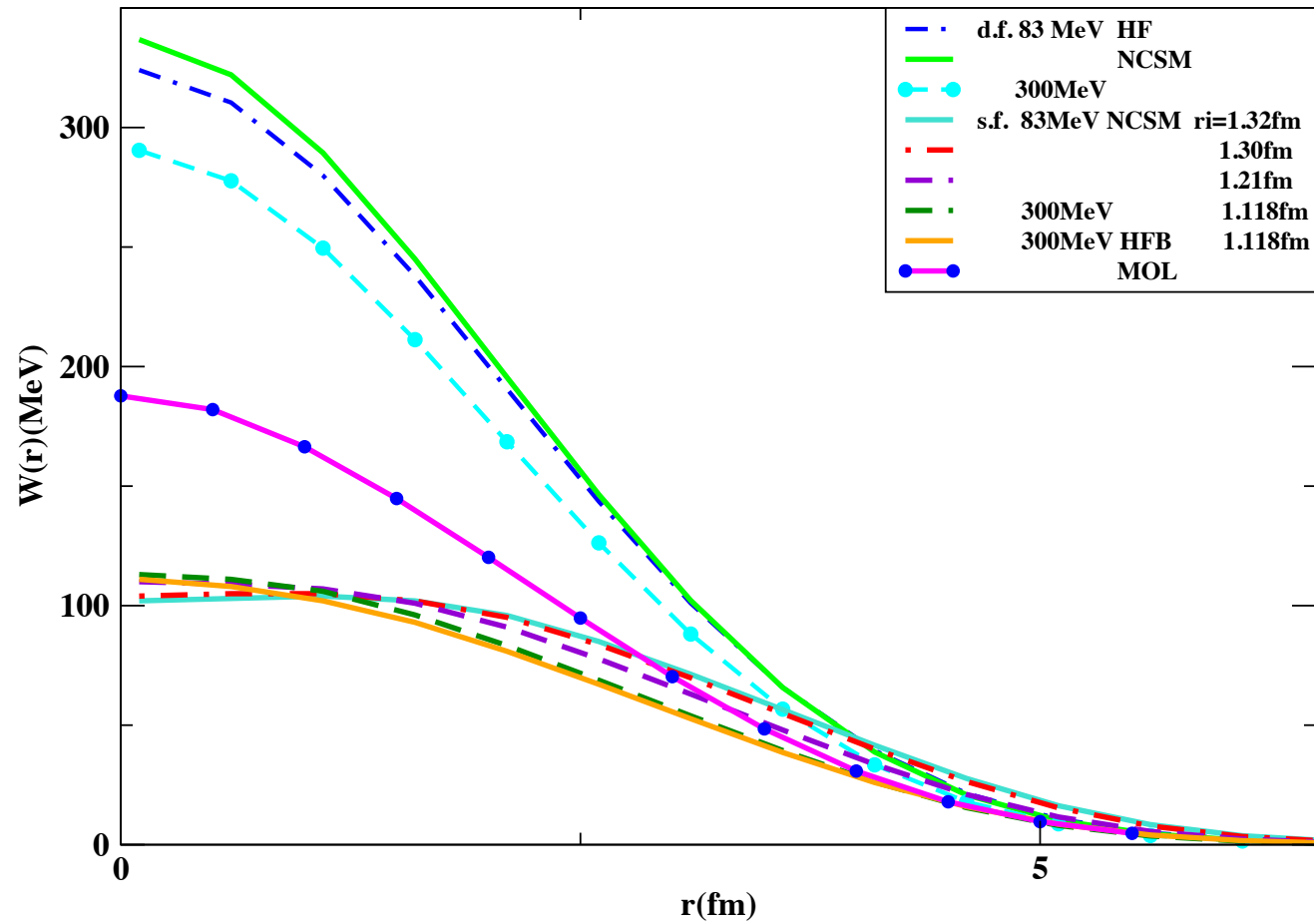
NCSM M. Vorabbi, et al., Phys. Rev. C103, 024604 (2021).

Thanks to Petr Navratil and Michael Gennari for providing the numerical densities

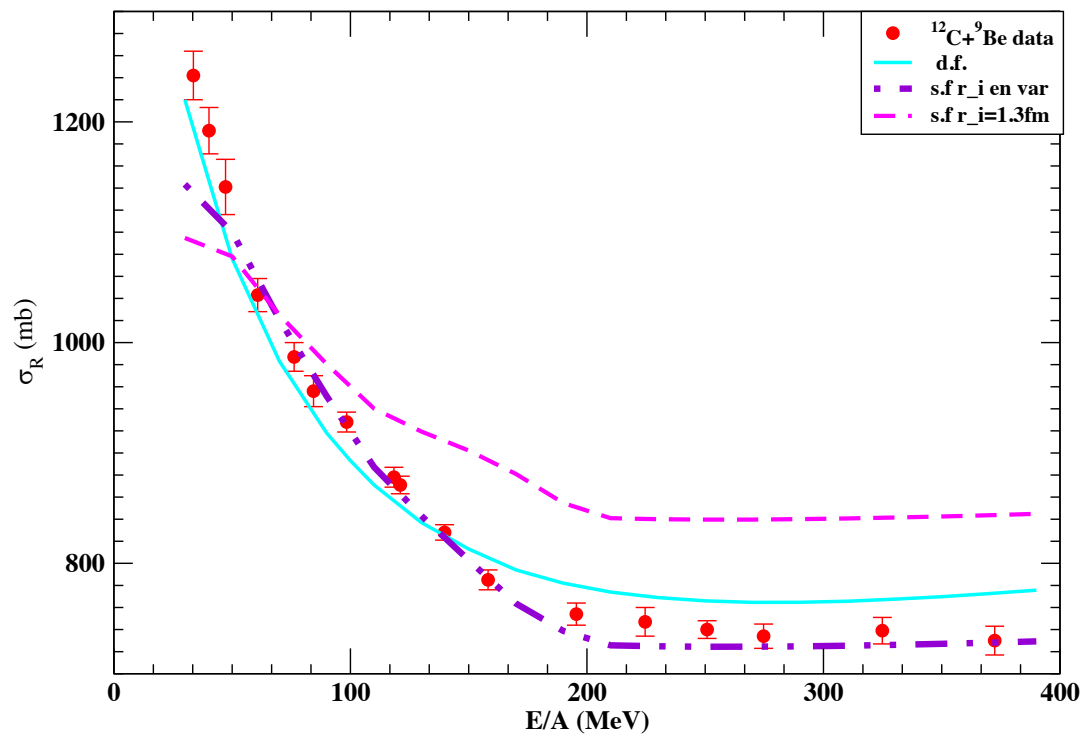
Also see Phys. Rev. C 99, 044603 (2019)
M. Burrows, Ch. Elster et al.,



D.F. vs S.F. for NN potentials

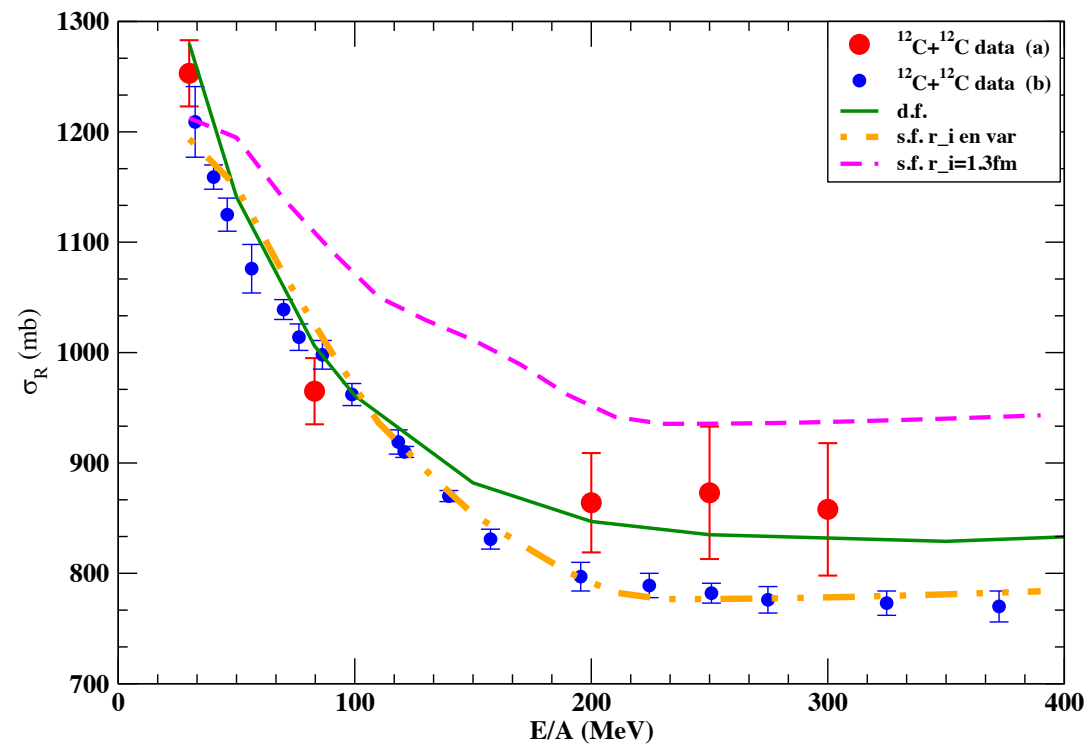


Data from Takechi et al. cf slide 5, Kox
 In d.f. $\sigma_{np,pp}$ from De Conti&Bertulani
 PRC81.064603 (2010).



| E_{lab} (MeV) | $r_i(^9Be)$ (fm) | $r_i(^{12}C)$ (fm) |
|----------------------------|-----------------------|------------------------|
| $30 \leq E_{lab} \leq 160$ | $1.4 - 0.0015E_{lab}$ | $1.32 - 0.0013E_{lab}$ |
| $E_{lab} > 160$ | 1.15 | 1.118 |

TABLE III: Energy-dependent optical-model parameter r_i for the (AB) potential for $n+^9Be$ and $n+^{12}C$



$^{12}\text{C}+^{12}\text{C}$

| E_{inc} (MeV) | model | r_s (fm) | $J_W/A_P A_T$ (MeVfm ³) | r.m.s (fm) | σ_{NCSM} (mb) | r.m.s (mb) | σ_{HF} (mb) | r.m.s | σ_{HFB} |
|--------------------|-------|---------------|--|---------------|-------------------------|---------------|-----------------------|-------|----------------|
| 83 | S.F. | 1.2 | 184 | 3.72 | 994 | 3.75 | 1008 | 3.78 | 1025 |
| | D.F. | 1.22 | 279 | 3.29 | 957 | 3.36 | 995 | 3.43 | 1027 |
| 300 | S.F. | 1.18 | 151 | 3.57 | 760 | 3.60 | 768 | 3.64 | 780 |
| | D.F. | 1.11 | 241 | 3.29 | 791 | 3.36 | 815 | 3.43 | 842 |

280A.MeV

$^{12}\text{Ne}+^{12}\text{C}$

| E_{inc} (MeV) | model | r_s (fm) | σ_{theo} (mb) | σ_{exp} (mb) | Nucleus | model | r_s (fm] | σ_{theo} (mb) | σ_{exp} (mb) | $r.m.s.$ (fm) |
|-----------------|-------|-------------|----------------------|---------------------|------------------|------------|------------------|----------------------|---------------------|---------------|
| 30 | S.F. | (1.35) 1.33 | (1478) 1456 | 1550 ± 75 | ^{42}Ca | S.F. | (1.23)1.14 | (1598) 1388 | 1463(13)(6) | 3.38 |
| | D.F. | 1.37 | 1560 | | | D.F. | 1.16 | 1460 | | |
| | 100 | S.F. | (1.27) 1.23 | | (1327)1211 | 1161 ± 80 | ^{43}Ca | S.F. | (1.22)1.14 | (1614)1402 |
| D.F. | | 1.21 | 1206 | D.F. | 1.17 | | | 1476 | | |
| 200 | | S.F. | (1.21)1.11 | (1193) 1012 | 1123 ± 80 | | ^{44}Ca | S.F. | (1.23)1.15 | (1630) 1417 |
| | D.F. | 1.15 | 1079 | D.F. | | 1.16 | | 1490 | | |
| | 300 | S.F. | (1.21)1.12 | (1181)1001 | | 1168 ± 100 | ^{46}Ca | S.F. | (1.24)1.15 | (1683)1466 |
| D.F. | | 1.13 | 1062 | D.F. | 1.17 | | | 1543 | | |
| | | | | | | | ^{48}Ca | S.F. | (1.23)1.16 | (1714)1495 |
| | | | | | | D.F. | 1.18 | 1573 | | |

Conclusions

- We have derived excellent $n+{}^9\text{Be}$, $n+{}^{12}\text{C}$ phenomenological optical potentials up to 500MeV, cross checked vs DOM.
- Also excellent single folding P (Core)-T OP validated for ${}^{12}\text{C} + {}^{12}\text{C}$, ${}^{12}\text{C}+{}^9\text{Be}$.
- Dominance of surface absorption (r_i decreases with energy).
- S.F. less ambiguous than D.F. (needs to fix a smaller n of parameters).
- Evolution of D.F. via nN *ab-initio*?

Jul 24 – 28. 2017



Best wishes
Congratulations!

M. Fukuda et al., private communication; D. Nishimura
et al., Osaka University Laboratory of Nuclear Studies (OULNS)
Annual Report 2006, p. 37.

| E_{lab} (MeV/nucleon) | σ_{exp} (mb) | $\sigma_{\text{d.fold}}^{\text{VMC}}$ (mb) | $\sigma_{\text{d.fold}}^{\text{HF}}$ (mb) | $\sigma_{\text{s.fold}}$ (mb) | $\sigma_{\text{s.fold}}^{+\text{surf}}$ (mb) | $\sigma_{\text{JLM}}^{\text{bare}}$ (mb) | $\sigma_{\text{JLM}}^{\text{ren}}$ (mb) | N_{JLM} | W_{surf} (MeV) | R_s (fm) | R_s^{fit} (fm) | a^{fit} (fm) | r_s (fm) |
|-----------------------------------|-------------------------------|---|--|----------------------------------|---|---|--|------------------|----------------------------|---------------|----------------------------|--------------------------|---------------|
| 20 | | 1267 | 1409 | 1078 | 1565 | 1338 | 1538 | 1.65 | 0.8 | 6.12 | 6.25 | 1.01 | 1.47 |
| 38 | | 1086 | 1191 | 1112 | 1341 | 1250 | 1324 | 1.20 | 0.5 | 5.95 | 5.99 | 0.97 | 1.44 |
| 40.9 | 1216 ± 57 | 1064 | 1166 | 1117 | 1291 | 1235 | 1215 | 0.95 | 0.4 | 5.95 | 5.99 | 0.98 | 1.44 |
| 43 | | 1050 | 1148 | 1103 | 1275 | 1221 | 1260 | 1.10 | 0.4 | 5.95 | 5.99 | 0.99 | 1.44 |
| 43.6 | 1269 ± 22 | 1046 | 1144 | 1106 | 1235 | 1219 | 1257 | 1.10 | 0.3 | 5.82 | 5.70 | 0.80 | 1.40 |
| 59 | | 960 | 1042 | 1047 | 1124 | 1130 | 1111 | 0.95 | 0.2 | 5.70 | 5.64 | 0.82 | 1.36 |
| 61.1 | 1104 ± 20 | 950 | 1030 | 1045 | 1122 | 1119 | 1119 | 1.00 | 0.2 | 5.68 | 5.63 | 0.83 | 1.36 |
| 66 | | 928 | 1006 | 1028 | 1066 | 1091 | 1028 | 0.85 | 0.1 | 5.60 | 5.55 | 0.80 | 1.35 |
| 67.4 | 1074 ± 32 | 923 | 999 | 1026 | 1056 | 1087 | 1087 | 1.00 | 0.08 | 5.60 | 5.53 | 0.80 | 1.35 |
| 68.3 | 1064 ± 16 | 919 | 995 | 1024 | 1052 | 1082 | 1063 | 0.95 | 0.075 | 5.55 | 5.49 | 0.80 | 1.33 |
| 83 | | 867 | 934 | 948 | 979 | 1015 | 987 | 0.93 | 0.015 | 5.40 | 5.38 | 0.78 | 1.29 |
| 84.9 | 981 ± 15 | 861 | 928 | 979 | 983 | 1008 | 989 | 0.95 | 0.01 | 5.40 | 5.36 | 0.80 | 1.29 |
| 95 | | 833 | 895 | 949 | 952 | 968 | 956 | 0.97 | 0.01 | 5.40 | 5.28 | 0.79 | 1.29 |
| 97.2 | 919 ± 24 | 827 | 888 | 949 | 951 | 963 | 923 | 0.90 | 0.005 | 5.35 | 5.28 | 0.80 | 1.28 |

Comparison with data, at low energy suggests the need to include the ${}^9\text{C}$ breakup channel explicitly

